Eur Radiol (2016) 26:4155–4161
DOI 10.1007/s00330-016-4263-0

HEAD AND NECK

Low-Dose CT of the Paranasal Sinuses: Minimizing X-Ray Exposure with Spectral Shaping

Wolfgang Wuest[1,2] · **Matthias May**[1] · **Marc Saake**[1] · **Michael Brand**[1] · **Michael Uder**[1] · **Michael Lell**[1]

Received: 16 June 2015 / Revised: 28 January 2016 / Accepted: 1 February 2016 / Published online: 24 February 2016

Abstract

Objectives Shaping the energy spectrum of the X-ray beam has been shown to be beneficial in low-dose CT. This study's aim was to investigate dose and image quality of tin filtration at 100 kV for pre-operative planning in low-dose paranasal CT imaging in a large patient cohort.

Methods In a prospective trial, 129 patients were included. 64 patients were randomly assigned to the study protocol (100 kV with additional tin filtration, 150mAs, 192x0.6-mm slice collimation) and 65 patients to the standard low-dose protocol (100 kV, 50mAs, 128 × 0.6-mm slice collimation). To assess the image quality, subjective parameters were evaluated using a five-point scale. This scale was applied on overall image quality and contour delineation of critical anatomical structures.

Results All scans were of diagnostic image quality. Bony structures were of good diagnostic image quality in both groups, soft tissues were of sufficient diagnostic image quality in the study group because of a high level of noise. Radiation exposure was very low in both groups, but significantly lower in the study group ($CTDI_{vol}$ 1.2 mGy vs. 4.4 mGy, $p < 0.001$).

Conclusions Spectral optimization (tin filtration at 100 kV) allows for visualization of the paranasal sinus with sufficient image quality at a very low radiation exposure.

✉ Wolfgang Wuest
wolfgang.wuest@uk-erlangen.de

[1] Radiological Institute, Friedrich-Alexander-University Erlangen-Nuremberg, Erlangen, Germany

[2] Radiological Institute, Maximiliansplatz 1, 91054 Erlangen, Germany

Key Points

- *Spectral optimization (tin filtration) is beneficial to low-dose parasinus CT*
- *Tin filtration at 100 kV yields sufficient image quality for pre-operative planning*
- *Diagnostic parasinus CT can be performed with an effective dose < 0.05 mSv*

Keywords Low dose · CT · Parasinus CT · Tin filtration · Spectral shaping

Introduction

Multidetector helical computed tomography (MDCT) is considered the standard modality for imaging of inflammatory disease in the paranasal sinuses, because of the high spatial resolution [1–4]. Computed tomography (CT) is frequently performed to diagnose or rule out sinusitis (both acute and chronic) and is used to differentiate mucosal disease patterns and, therefore, plan surgery. According to the current guidelines, it is mandatory before functional endoscopic sinus surgery (FESS) to visualize individual anatomic variants and extension of disease.

MDCT also provides the basis for planning the surgical approach, image-guided navigation, and robotic surgery [5, 6]. MDCT is also used in the setting of postoperative complications and follow-up.

Because paranasal imaging is often performed in young patients without life-limiting disease, and repetitive examinations may be required, radiation dose is of special concern. To adhere to the ALARA principle ("as low as reasonably achievable") different approaches to lower radiation exposure have been proposed, including orbital bismuth shielding to reduce direct radiation exposure of the eye lens or reducing tube voltage and

current [7, 8]. The high contrast between air and the bony walls of the paranasal sinuses allows reducing the tube current and acceptance of increased image noise to a certain degree without compromising the diagnostic accuracy [9–11]. Low-kV imaging is another strategy to effectively reduce dose, which recently gained popularity. Reducing the tube voltage necessitates an increase in tube current to keep the image noise level constant, but the attenuation of bone increases with lower kV settings, increasing the bone–air contrast [9].

Tin filtration was recently introduced in dual source CT systems, primarily to better separate the two energy spectra in dual-energy CT. The tin filter absorbs low-energy photons that are less relevant in a high-contrast setting (such as bone or lung imaging) and, therefore, reduces the radiation exposure of the patient.

We sought to investigate image quality and radiation dose of a protocol with tin filtration at 100 kV and to compare the results with a standard CT protocol.

Materials and methods

Phantom study

To evaluate the influence of different CT scanner geometries and hardware and the effect of tin filtration on image quality with comparable scan parameters, additional measurements with a 16-cm acrylic CT dose index (CTDI) phantom and the Gammex 464 were performed. Since tin filtration absorbs about 9/10 of the photons emitted from the X-ray tube, mAs settings had to be increased in the tin filtration protocol to obtain identical $CTDI_{vol}$. See Table 1 for an overview of the used scan parameters.

Patient study

Consecutive patients scheduled for paranasal sinus CT for suspected inflammatory mucosal disease were included. Patients scheduled for sinus CT with contrast medium (suspicion of abscess formation or tumour) and trauma evaluation were excluded. A total of 129 patients met the inclusion criteria. All patients signed informed consent; the study protocol was approved by the local institutional review board. Patients were randomly assigned to single-source CT (SSCT, standard protocol) or dual source CT (DSCT; study protocol). 64 patients (29 female and 35 male patients, mean age 49 ± 18 years, range 10–88 years) were assigned to the study protocol performed on a third-generation DSCT system (Somatom FORCE, Siemens, Forchheim, Germany) with the following parameters: 0.5-s gantry rotation time, 192 x 0.6-mm collimation using a z-flying focal spot, 150 mAs tube current at 100 kV tube voltage with tin (Sn) pre-filtration, tube current modulation switched off. This protocol was chosen based on the results of a previous phantom study [12].

Table 1 Overview of the used scan parameters in the phantom study

Scan protocol	AS+	FORCE	FORCE
kV	100	100	Sn100
mAs	50	50	508
Pitch	0.9	0.9	0.9
Reconstruction kernel	H30s	Hr38s	Hr38s
Collimation	128 × 0.6 mm	192 x 0.6 mm	192 x 0.6 mm
Slice thickness	3 mm	3 mm	3 mm
Rotation time	1 s	1 s	1 s
CTDIvol (mGy)	4.4	4.4	4.4

65 patients (28 female and 37 male patients, mean age 43 ± 16 years, range 14–80 years) were assigned to the control group, where the examination was performed on a SSCT system (Definition AS+, Siemens Healthcare, Forchheim, Germany) with the following parameters: 1-s gantry rotation time, 128 × 0.6-mm slice collimation using a z-flying focal spot, 50 mAs tube current at 100 kV tube voltage, tube current modulation switched off (CareDose4D).

In both groups, patient position was supine with a slight reclination of the head to obtain a parallel alignment of the upper jaw to the gantry, to minimize artefacts from dental hardware. The scan range included the roof of the frontal sinuses to the alveolar process of the maxillary sinus. 3-mm axial, 3-mm coronal as well as 3-mm sagittal images were reconstructed from the raw data set, using both bone and soft tissue kernels. Bf36d and Br64d were used as soft tissue and bone kernel in DSCT, H30s and H70h in SSCT. Additionally, thin slices in axial orientation (0.6-mm slice thickness, 0.5-mm increment) were reconstructed for multiplanar reformation evaluation and transferred to a 3D workstation (SyngoVia VA30A, Siemens Healthcare, Forchheim, Germany). No iterative reconstruction algorithms were used for image reconstruction.

Subjective image quality

Parameters were evaluated independently by two radiologists blinded to all clinical data. Image quality was assessed using a five-point Likert scale: 1, non-diagnostic; 2, limited diagnostic value with substantial image noise and artefacts; 3, diagnostic, sufficient image quality; 4, diagnostic, good image quality; and 5, diagnostic, excellent image quality. This scale was applied on overall image noise and diagnostic acceptability of mastoid cells, carotid canal at the skull base, lamina papyracea, lamina cribrosa, bony septae of the ethmoid cells, uncinate process, nasal conchae, eye bulb, eye muscles, retrobulbar fat and optic nerve. The overall rating for each protocol was defined by the worst rating of these structures. Mucosal structures of the maxillary, ethmoid,

frontal and sphenoid sinuses were also evaluated. Mucosal thickening was any thickening of more than 4 mm in at least one wall of the sinuses.

Objective image quality

To obtain and compare objective parameters between the two acquisition protocols, regions of interest (ROIs) were placed on axial 3-mm soft tissue reconstructions in both eye globes, in the retrobulbar fat and in the maxillary sinus. ROIs with at least an area of 2 mm^2 were measured to obtain attenuation values (a). Standard deviations (SDs) of these measurements were considered as image noise (n) and contrast to noise ratios (CNRs) were calculated by division of attenuation differences between eye globes and air as well as retrobulbar fat and eye globes with image noise according to the equation: CNR = (a1-a2)/n. "n" always corresponds to the average image noise of the first mentioned structure in the CNR formula.

To account for anatomic differences between patients, the ROIs were chosen as large as possible, while carefully avoiding image artefacts and adjacent structures in order to prevent partial volume effects.

Estimation of radiation exposure

The estimation of the effective radiation dose associated with the CT examination was based on the dose–length product (DLP) and calculated using the following formula according to International Commission on Radiological Protection Publication 103 (ICRP 103): DLP [mGy x cm] x 0.0019 [mSv x mGy^{-1} x cm^{-1}] [13]. DLP values were derived from the patient protocol. Because the Sn100kV examinations are referenced to a 32-cm phantom in the patient protocol, the values had to be converted to match the 16-cm phantom [13]. The respective conversion factor for the CT system used in this study was 2.5.

Statistical analysis

Values are given as the mean ± SD or as the median. Mann–Whitney U testing was performed for radiation exposure comparison between both groups and for comparison of subjective and objective image quality. Inter-rater and intra-rater agreement was assessed using Cohen's kappa test; kappa values >0.41 were interpreted as moderate; kappa-values >0.61 as substantial; and kappa-values >0.81 as almost perfect agreement according to Landis and Koch [14].

Significance levels of 0.05 were assumed. Statistical analysis was performed using software (SPSS Statistics, Version 19, SPSS Inc./IBM, Chicago, IL, USA).

Results

Phantom study

For all phantom scans, $CTDI_{vol}$ was identical (4.4 mGy). Using 100 kV and 50 mAs for the 16-cm acrylic CTDI phantom, image noise was significantly lower with DSCT as compared to SSCT (12 ± 0.6 vs.11 ± 0.6, $p < 0.05$). Using 100 kV with tin filtration and 508 mAs, image noise was even lower (10 ± 0.6, $p < 0.05$, see Fig. 1). Removing the low-energy photons from the 100-kV spectrum with tin filtration affected the mean attenuation [134 ± 3 Hounsfield units (HU)] compared to identical values without tin filtration on both CT systems (118 ± 3 HU DSCT and 118 ± 2 HU SSCT).

See Table 2 for the Gammex 464 results.

Patient study

Overall image quality was rated diagnostic by the readers in all patients; no study had to be repeated.

In the study group, 40/62 patients had mucosal disease, 8 patients had prior surgery and recurrent mucosal swelling; in 22 patients, mucosal disease was ruled out.

In the control group, 51/65 patients had mucosal disease, 6 patients had prior surgery and recurrent mucosal swelling, and in 14 patients, mucosal disease was ruled out.

For the nasal conchae, uncinate process and the bony septae of the ethmoid cells, subjective image quality was comparable between the study and control group. For all other soft-tissue and bone-containing structures, image quality was different between both groups. For detailed results, see Table 3.

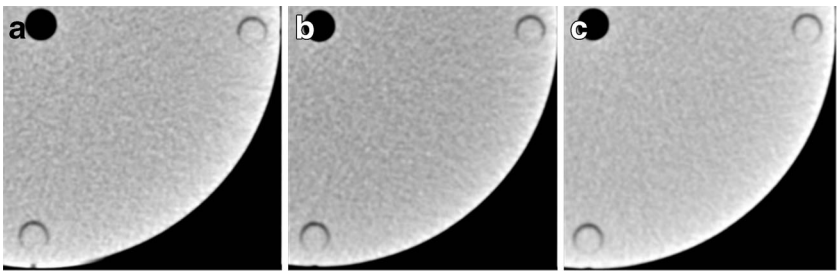

Fig. 1 Image examples of the phantom study for *A*) SSCT with 100 kV and 50 mAs, *B*) DSCT with 100 kV and 50 mAs and *C*) DSCT with Sn100kV and 508 mAs. Reduced image noise using DSCT with tin filtration compared to the other protocols with identical $CTDI_{vol}$

Table 2 Mean attenuation and standard deviation of the evaluated structures in the phantom study using the Gammex 464

Scan protocol	AS+		FORCE		FORCE	FORCE
kV	100		100		Sn100	Sn100
mAs	50		50		508	508
	Mean attenuation	Standard deviation	Mean attenuation	Standard deviation	Mean attenuation	Standard deviation
Polyethylene	−101	16	−107	12	−50	11
Bone	1069	20	1132	31	907	18
Water	0	15	1	12	2	12
Acrylic	134	16	136	13	151	12
Air	−1023	1	−1023	2	−1023	2

Bony structures (mastoid cells, nasal conchae etc.) were diagnostic with good image quality in both groups, soft tissues (optic nerve, retrobulbar fat etc.) were diagnostic with sufficient image quality in the study group because of a high level of noise.

CNR values (eye globe/air and retrobulbar fat/eye globe) were higher for the control group (92 ± 21 vs. 69 ± 11 and 11 ± 3 vs. 6 ± 1). See Table 4 for HU and noise measurements.

Examples of typical cases are given in Figs. 2, 3, and 4.

Study group

Image quality of soft tissue structures (optic nerve, retrobulbar fat etc.) were sufficient (median score = 3). Mastoid and bony septae of the ethmoid cells, nasal conchae and uncinate process were rated excellent (median score = 5) and all other structures good (median score = 4). Contour delineation of the lamina cribrosa, the most delicate structure of this evaluation, was good.

Inter- and intra-rater agreement for all evaluated structures is given in Table 3.

Control group

Mastoid cells, bony septae of the ethmoid cells, nasal conchae, uncinate process and retrobulbar fat were rated excellent (median = 5). All other structures were rated good (median = 4). Contour delineation of the lamina cribrosa, the most delicate structure of this evaluation, was also rated good (median = 4).

Inter- and intra-rater agreement for all evaluated structures is given in Table 3.

Radiation exposure

Radiation exposure was very low in both groups, but significantly lower in the study group ($CTDI_{vol}$ 1.2 mGy vs. 4.4 mGy, $p < 0.001$).The mean effective dose of the study

Table 3 Subjective image quality for all evaluated anatomic landmarks. Values are given as mean ± standard deviation

	Study group				Control group				
	Reader 1	Reader 2	Inter-rater kappa value	Intra-rater kappa value	Reader 1	Reader 2	Inter-rater kappa value	Intra-rater kappa value	*p* value
Image quality	3.2 ± 0.4	3.2 ± 0.5	0.88	0.86	4.2 ± 0.4	4.2 ± 0.4	0.89	0.85	<0.05*
Image noise	3.6 ± 0.6	3.9 ± 0.6	0.61	0.64	4.2 ± 0.4	4.2 ± 0.4	0.68	0.65	<0.05*
Mastoid cells	4.5 ± 0.7	4.5 ± 0.7	0.88	0.81	4.9 ± 0.2	4.9 ± 0.3	0.78	0.80	<0.05*
Lamina papyracea	3.9 ± 0.6	4 ± 0.7	0.66	0.65	4.5 ± 0.5	4.6 ± 0.5	0.65	0.61	<0.05*
Carotid canal	3.8 ± 0.6	3.9 ± 0.8	0.64	0.61	4.2 ± 0.4	4.2 ± 0.3	0.57	0.60	<0.05*
Lamina cribrosa	3.7 ± 0.6	3.6 ± 0.7	0.52	0.67	4.3 ± 0.5	4.3 ± 0.5	0.65	0.69	<0.05*
Nasal concha	4.8 ± 0.5	4.7 ± 0.5	0.85	0.84	4.8 ± 0.4	4.9 ± 0.4	0.86	0.82	0.9
Uncinate process	4.4 ± 0.8	4.5 ± 0.7	0.82	0.81	4.6 ± 0.5	4.7 ± 0.5	0.85	0.82	0.2
Bony septae of ethmoid cells	4.5 ± 0.8	4.4 ± 0.7	0.81	0.80	4.6 ± 0.6	4.7 ± 0.6	0.80	0.84	0.2
Eye bulb	3.2 ± 0.5	3.5 ± 0.6	0.64	0.61	4 ± 0.3	3.9 ± 0.4	0.71	0.64	<0.05*
Eye muscles	3.4 ± 0.5	3.6 ± 0.5	0.64	0.68	4.5 ± 0.5	4.4 ± 0.4	0.71	0.68	<0.05*
Retrobulbar fat	3.3 ± 0.5	3.5 ± 0.6	0.61	0.64	4.8 ± 0.4	4.6 ± 0.5	0.60	0.68	<0.05*
Optic nerve	3.4 ± 0.5	3.6 ± 0.5	0.57	0.62	4.5 ± 0.5	4.4 ± 0.5	0.66	0.65	<0.05*

Table 4 Mean attenuation and standard deviation of the evaluated structures in the patient study

	AS+		FORCE	
	Mean attenuation	Standard deviation	Mean attenuation	Standard deviation
Eye bulb	28	12	6	15
Retrobulbar fat	−108	13	−80	15
Air	−1021	3	−976	13

protocol (tin filtration) was 0.04 ± 0.002 mSv (after conversion) and 0.1 ± 0.02 mSv in the control group ($p < 0.001$). DLP values were 22.5 mGycm (after conversion) in the study group vs. 58 mGycm in the control group.

Discussion

In a recently published phantom study, a systematic evaluation of scan protocols to optimize image quality and radiation exposure on a third-generation DSCT was performed [12]. CT protocols with different tube voltage (70–150 kV), current (25–300 mAs), pre-filtration, pitch value, and rotation time were assessed. 100 kV with tin filtration and 150 mAs has been suggested to be the best compromise between dose and image quality for pre-operative sinus surgery.

We could confirm this in a large patient cohort. Pre-operative diagnostic CT of the paranasal sinuses is feasible with diagnostic image quality and very low radiation exposure (0.04 mSv), using 100 kV and tin filtration. All landmarks were sufficiently visualized and diagnostic confidence was maintained, although subjective and objective image quality was rated higher in the control group.

Image quality is influenced by a number of factors. For example, kV and mAs settings are two factors that affect the number of X-rays detected and by that influence, image noise. Image noise is also profoundly altered by reconstruction filters. As shown in the phantom using identical scan protocols, third-generation DSCT enables scanning with reduced image noise compared to SSCT, which could be attributable to a different detector efficiency. Image noise was even further reduced with tin filtration at similar $CTDI_{vol}$. By absorbing 9/10 of the photons emitted from the X-ray tube, tin filtration narrows and shifts the X-ray spectrum towards higher keV levels, which explains lower image noise and higher attenuation values. Spectral shaping allows for scanning at dose levels substantially below the lower limit of recent CT systems. Using conventional pitch values, $CTDI_{vol}$ of 1.2 mGy is not available in protocols at 100 kV without tin pre-filtration on both CT systems used in our study. Image quality at comparable $CTDI_{vol}$ values at 70 kV was associated with strongly impaired image quality, mainly due to the low-energy spectra.

Because many young patients are scheduled for CT of the paranasal sinuses, dose reduction and, by that, image noise reduction is an issue. Although the risk of cancer induction may not be considered relevant for such low X-ray exposure,

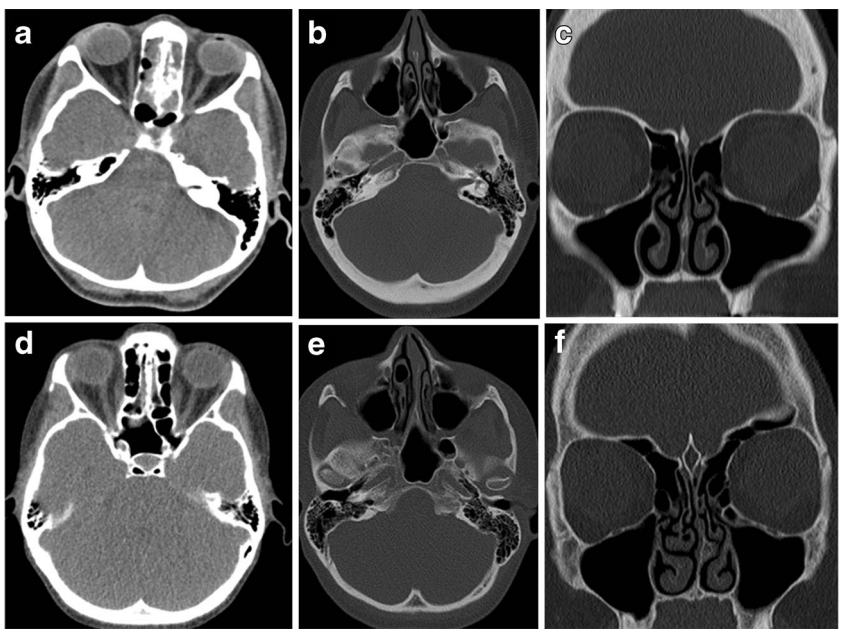

Fig. 2 Images of the control group in the upper row (*A–C*) and of the study group in the lower row (*D–F*), 3-mm slice thickness. Bony structures are clearly definable in both groups with higher image noise in the study group

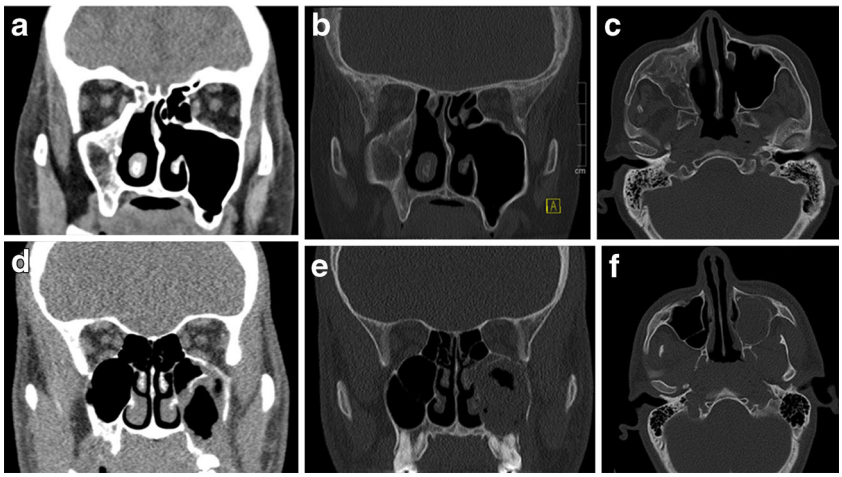

Fig. 3 Images of the control group in the upper row (*A–C*) and of the study group in the lower row (*D–F*), 3-mm slice thickness. Chronic sinusitis was observed in both cases, but higher image noise using tin filtration

deterministic effects associated with radiation exposure of the eye lenses are of concern especially with repetitive examinations. A number of studies suggest there may be significant risk of cataract in populations exposed to low doses of ionizing radiation [15–17]. Cataracts have been considered to be a deterministic effect with a threshold of 0.5–2 Gy on a short-term base [18]. The risk of radiation-induced malignant neoplasms of the thyroid gland is based on a stochastic risk, on the order of 0.0075 per Gray [19].

On the other hand, the risk of missing a present abnormality by applying dose reduction may be of even greater relevance than the projected risk of radiation-induced adverse effects in the future. This issue was termed the "second risk of radiation" by Cohen [20]. The trade-off between image quality and dose must, therefore, be well-balanced to avoid a negative impact on diagnostic accuracy.

Alternative imaging techniques include plain X-ray images, cone-beam CT (CBCT) with flat panel detectors or magnetic resonance imaging (MRI). For the complex anatomy of the paranasal sinus, projection radiography is not sufficient and despite lower costs compared to other imaging modalities, should, therefore, be avoided whenever possible [5, 21]. CBCT is increasingly used for imaging of the paranasal sinus because of lower cost and relatively low radiation exposure. The downside of CBCT systems are longer acquisition times, inadequate soft tissue resolution, fixed scan field of view (FOV), cone beam artefacts in image reconstruction and relatively long image reconstruction time. MRI can also be used for exclusion of inflammatory sinusoidal disease without any radiation exposure. However, due to inferior visualization of the fine bony structures, higher cost and longer examination time, this modality is used only in specific situations.

A major limitation of this study is the use of two different CT scanners which affects image quality, as demonstrated in the phantom study. Our primary aim was to verify a previously proposed scan protocol in a clinical setting in a large patient cohort and to compare the results with our standard low dose protocol.

Another limitation is that tin filtration is not available in the vast majority of CT systems at the moment. Image quality of the proposed protocol was considered to be sufficient to detect or rule out sinusitis, to provide relevant anatomic information for surgery and allow 3D surgical navigation. We did not include patients with other indications like trauma or cerebrospinal fluid (CSF) leakage, where additional soft tissue evaluation is necessary. We also did not investigate the potential of iterative reconstruction techniques; however, they seem to negatively affect the detailed delineation of bony structures [22].

In conclusion, we could demonstrate that CT of the paranasal sinuses can be performed at very low radiation exposure

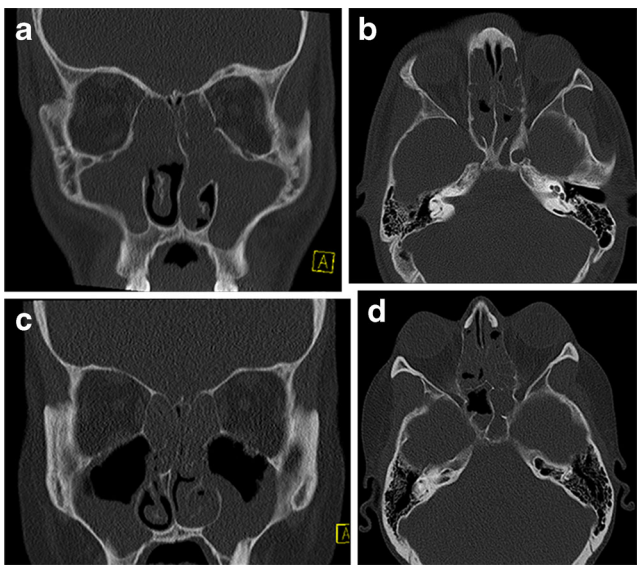

Fig. 4 Images of the control group in the upper row (*A–B*) and of the study group in the lower row (*C–D*), 3-mm slice thickness. Sinusitis was observed in both cases with bony septae of the ethmoid cells and lamina papyracea still definable

maintaining high image quality for the diagnosis of sinusitis and pre-operative planning using 100 kV and tin-filtration.

Acknowledgments The scientific guarantor of this publication is Wolfgang Wuest. The authors of this manuscript declare no relationships with any companies whose products or services may be related to the subject matter of the article. The authors state that this work has not received any funding. One of the authors has significant statistical expertise. Institutional review board approval was obtained. Written informed consent was obtained from all subjects (patients) in this study. Methodology: prospective, randomised controlled, performed at one institution.

References

1. Hopper RA, Salemy S, Sze RW (2006) Diagnosis of midface fractures with CT: what the surgeon needs to know. Radiographics 26: 783–793
2. Duvoisin B, Landry M, Chapuis L, Krayenbuhl M, Schnyder P (1991) Low-dose CT and inflammatory disease of the paranasal sinuses. Neuroradiology 33:4036
3. Tack D, Widelec J, De Maertelaer V, Bailly JM, Delcour C, Gevenois PA (2003) Comparison between low-dose and standard-dose multidetector CT in patients with suspected chronic sinusitis. AJR Am J Roentgenol 181:939–944
4. Kaur J, Chopra R (2010) Three dimensional CT reconstruction for the evaluation and surgical planning of mid face fractures: a 100 case study. J Maxillofac Oral Surg 9:323–328
5. Abul-Kasim K, Strombeck A, Sahlstrand-Johnson P (2009) Low-dose computed tomography of the paranasal sinuses: radiation doses and reliability analysis. Am J Otolaryngol 32:47–51
6. Hoang JK, Eastwood JD, Tebbit CL, Glastonbury CM (2010) Multiplanar sinus CT: a systematic approach to imaging before functional endoscopic sinus surgery. Am J Roentgenol 194: W527–W536
7. Perisinakis K, Raissaki M, Theocharopoulos N, Damilakis J, Gourtsoyiannis N (2005) Reduction of eye lens radiation dose by orbital bismuth shielding in pediatric patients undergoing CT of the head: a Monte Carlo study. Med Phys 32:1024–1030
8. Hein E, Rogalla P, Klingebiel R, Hamm B (2002) Low-dose CT of the paranasal sinuses with eye lens protection: effect on image quality and radiation dose. Eur Radiol 12:1693–1696
9. Brem MH, Zamani AA, Riva R et al (2007) Multidetector CT of the paranasal sinus: potential for radiation dose reduction. Radiology 243:847–852
10. Hagtvedt T, Aalokken TM, Notthellen J, Kolbenstvedt A (2003) A new low-dose CT examination compared with standard-dose CT in the diagnosis of acute sinusitis. Eur Radiol 13:976–980
11. Hojreh A, Czerny C, Kainberger F (2005) Dose classification scheme for computed tomography of the paranasal sinuses. Eur J Radiol 56:31–37
12. Wuest W, May MS, Brand M, Bayerl N, Krauss A, Uder M, Lell M (2015) Improved Image Quality in Head and Neck CT Using a 3D Iterative Approach toReduce Metal Artifact. AJNR Am J Neuroradiol 36(10):1988–93
13. Deak PD, Smal Y, Kalender WA (2010) Multisection CT protocols: sex- and age-specific conversion factors used to determine effective dose from dose-length product. Radiology 257:158–166
14. Landis JR, Koch GG (1977) The measurement of observer agreement for categorical data. Biometrics 33:159–174
15. Klein BE, Klein R, Linton KL, Franke T (1993) Diagnostic x-ray exposure and lens opacities: the Beaver Dam Eye Study. Am J Public Health 83:588–590
16. Chodick G, Bekiroglu N, Hauptmann M et al (2008) Risk of cataract after exposure to low doses of ionizing radiation: a 20-year prospective cohort study among US radiologic technologists. Am J Epidemiol 168:620–631
17. Yuan MK, Tsai DC, Chang SC et al (2013) The risk of cataract associated with repeated head and neck CT studies: a nationwide population-based study. AJR Am J Roentgenol 201:626–630
18. ICRP (2007) The 2007 Recommendations of the International Commission on Radiological Protection. ICRP Publication 103. 2007. Elsevier, Orlando
19. NCRP NCoRPaM (1985) Induction of thyroid cancer by ionizing radiation. NCRP report 80. NCRP Publications, Bethesda
20. Cohen MD (2009) Pediatric CT radiation dose: how low can you go? Am J Roentgenol 192:1292–1303
21. Aalokken TM, Hagtvedt T, Dalen I, Kolbenstvedt A (2003) Conventional sinus radiography compared with CT in the diagnosis of acute sinusitis. Dentomaxillofac Radiol 32:60–62
22. Hoxworth JM, Lal D, Fletcher GP et al (2014) Radiation dose reduction in paranasal sinus CT using model-based iterative reconstruction. AJNR Am J Neuroradiol 35:644–649